RESEARCH ARTICLE

On-line Configuration Identification and Control of Modular Reconfigurable Flight Array

Bin Ren[1,2], **Jianhui Liu**[1,2], **Simin Zhang**[1,2], **Chunxi Yang**[1,2,*] **and Jing Na**[1,2]

[1] Faculty of Mechanical and Electrical Engineering, Kunming University of Science and Technology, Kunming 650500, China

[2] Yunnan Key Laboratory of Intelligent Control and Application, Kunming University of Science and Technology, Kunming 650500, China

Abstract

With the increasing complexity of the working environment and the diversification of mission requirements of UAVs, traditional UAVs have a fixed structure and single function. It is difficult to be applied in occasions with complex environments and changing load demands. The modular reconfigurable flight array (MRFA) is composed of no less than four isomorphic unit modules that are freely spliced together. By adding or removing flight unit modules and adjusting the arrangement of flight unit modules, the configuration of the MRFA can be changed, so that it can adapt to complex environments and then complete different flight missions. In the process of MRFA research and development, online configuration identification has become one of important problems to be solved. In this paper, a configuration recognition algorithm is designed based on the breadth-first searching method to identify the online structure of MRFA firstly. Then, the dynamic model of the aircraft is carried out according to the obtained configuration information. At the same time, the mathematical model and configuration information of the MRFA are combined to establish an optimization control allocation mechanism to allocate suitable rotational speed for multiple rotors. Finally, several examples are carried out to show that the proposed technology can recognize the configuration with 100% recognition rate and average online recognition time 569.4ms. Then a cascade PID controller is designed to realize the flight control of the irregular MRFA with faster tracking performance of no more than 40 seconds.

Keywords: modular reconfigurable flight array, breadth-first search, configuration recognition, dynamic modeling, control allocation.

1 Introduction

In recent years, Rotor UAVs have been widely used in large scale fields such as coaxial drones [1], omnidirectional heterogeneous UAV [2] and UAV swarm [3] because of their higher efficiency, better flexibility and high security. However, in practice, UAVs with different performance will be selected

Academic Editor:
Feng Ding

Submitted: 15 September 2024
Accepted: 26 September 2024
Published: 29 September 2024

Vol. 1, **No.** 2, 2024.
10.62762/TIS.2024.681878

***Corresponding author:**
Chunxi Yang
ycx@kmust.edu.cn

Citation
Ren, B., Liu, J., Zhang, S., Yang, C., & Na, J. (2024). On-line Configuration Identification and Control of Modular Reconfigurable Flight Array. *ICCK Transactions on Intelligent Systematics*, 1(2), 91–101.

© 2024 ICCK (Institute of Central Computation and Knowledge)

according to task requirements, such as endurance time, load capacity, maneuverability and size of UAVs. In order to make UAVs have better applicability to the various environment and diverse task requirements, scholars have proposed a class of special UAVs based on modular design conception [4–6]. The modular UAVs design the unit flight module with the same shape and control system based on the modular conception. By splicing multiple module units, the special UAVs with different shapes and functions are combined to realize the multi-functional requirements of the rotor UAV [7].

Carlson et al. [8] designed a modular reconfigurable air vehicle based on a composite rotorcraft. The idea of modular splicing increased the planar aspect ratio of the vehicle's wings to achieve a longer flight time. In the Bionics and Robotics Laboratory at the University of Nevada, Reno designed a modular aerial vehicle based on articulated joints was designed [9], which achieves in-flight deformation. Ryll et al. [10, 11] designed a deformable six-rotor-FAST-Hex based on the rotor module, which can be arbitrarily switched from over-actuated by changing the configuration of the number of rotors. Inspired by the literature [7], we designed a modular reconfigurable flight array based on the modular conception, which can be reconfigured arbitrarily in its configuration.

The modular reconfigurable flight array (MRFA) is formed by splicing multiple homogeneous unit modules, and the dynamic models of the flight array corresponding to different configurations are also different. Therefore, it is very important to design an online algorithm that can identify the position and overall configuration of each unit module in the flight array, and finally determine the dynamic model of the reconfigurable flight array.

Similar online topology identification methods have been widely studied in reconfigurable robots. Among them, the configuration recognition method based on directed graph is used to describe the connection state and interface information of modular robots [12]. Yang et al. [13] introduced a modular reconfigurable flight array platform and established a dynamics model with a corresponding control allocation matrix to map control inputs to individual module actuators, providing a foundation for configuration-dependent flight control of reconfigurable flight arrays.

However, although these studies have made significant progress in the field of modular robotics, these methods cannot be effectively applied to the configuration identification of flying arrays. Furthermore, to achieve high maneuverability flight control of modular reconfigurable flight arrays, the relationship between topological configurations and dynamical models needs to be established. A fast modelling method is also developed to achieve smooth flight of reconfigurable flight arrays with different configurations.

Motivated by these researches mentioned above, we combined with the configuration identification method of modular robot and the characteristics of modular reconfigurable flight array, the online identification algorithm of flight array configuration is designed based on the breadth-first search method, and then the cascade PID controller is used to control the dynamic model based on the identification information of the algorithm. Finally, the smooth flight of modular reconfigurable flight array is shown in the given example.

2 Hardware structure design of MRFA

2.1 Structural design

The modular reconfigurable flight array is composed of multiple unit modules with the same frame structure, so that it has the characteristics of variable structure. Each unit module consists of a carbon braided base plate, a communication module circuit top plate, a brushless motor, a propeller, and a connecting mechanism which can be seen in Figure 1.

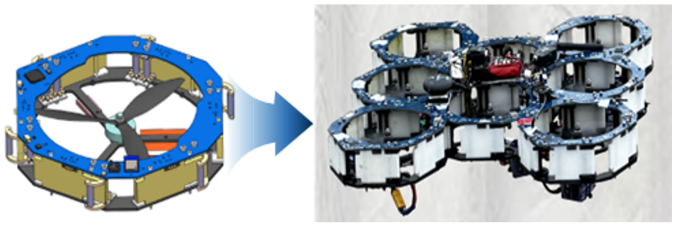

Figure 1. Modular reconfigurable flight array.

The shape of the flight unit module in Figure 1 is a six-prism. It is noticed that the connecting mechanism is installed on each elevation of the unit module, which is convenient for the connection of the connecting mechanism between different modules, and realizes the rapid splicing and splitting of multiple flight unit modules. Through the arbitrary splicing of unit modules, aircrafts of different configurations can be combined, which greatly expands the functions and application scenarios than those of traditional aircrafts.

2.2 Hardware design of communication module

The change of the number and spatial position of the unit modules is the reason for the change of the modular reconfigurable flight array configuration and then the control allocation matrices of MRFA with different configurations are also different. In order to realize the automatic solution of the control allocation matrices of flight arrays with different configurations, the reconfigurable flight array is required to have the ability to quickly identify its own configuration, so as to quickly obtain the position information of each unit module in the whole flight array.

In this paper, the automatic acquisition of flight array configuration information is realized based on the connection information between each unit module. For this reason, the unit module shown in Figure 1 is designed. Among them, the communication module circuit board in the unit module is the main component to realize the configuration identification. UART serial port, I2C and Bluetooth communication are used to realize the information interaction and sharing between each unit module. The circuit connection frame is shown in Figure 2.

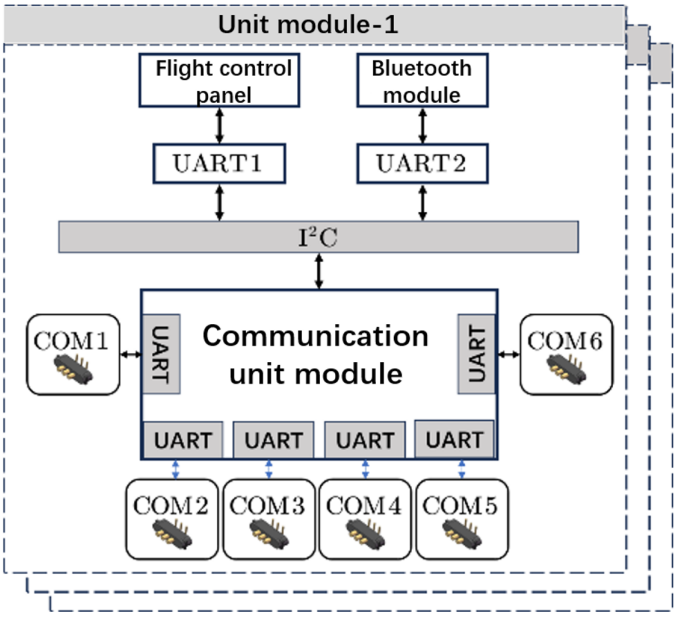

Figure 2. Unit module communication topology.

The unit module communication control board uses STM32F407 microcontroller, which is equipped with six serial communication ports, evenly distributed on the six connection surfaces of each unit module, and can interact with adjacent unit modules to identify the connection relationship between adjacent unit modules. I2C is used to expand the UART serial port, which is connected to the Bluetooth module and the flight control board respectively. The Bluetooth communication module is used to complete the information interaction between the modules and help the integration of the global connection information of the reconfigurable flight array. Finally, the global connection information is transmitted to the flight control board through UART1, and the global perception of the reconfigurable flight array configuration is realized.

3 Topology recognition of MRFA

In this section, we use a breadth-first search-based method to design an online configuration recognition algorithm, which is able to avoid the local optimum problem and ensure a comprehensive perception of the whole array, thus improving the accuracy of recognition. And the algorithm has low complexity and is suitable for real-time online recognition, which helps to enhance the adaptive ability and flexibility of flight arrays in dynamic environments. According to the algorithm, the topological configuration of MRFA can be obtained and applied to the establishment of the dynamic model.

The output distribution of each motor in reconfigurable flight array is closely related to its current configuration information. As shown in Figure 3, $E(j)_i$ represents the j-th connection surface in the i-th flight unit module in the communication module, where $i \in \{1, 2, \cdots, N\}$ represents the reconfigurable flight array unit module number, and N represents the total number of flight unit modules. $j \in \{1, 2, \cdots, 6\}$ is the connection surface number in the unit module. The connecting surface $E(1)_i$ is always corresponding to the UART1 serial port, and other surfaces are also corresponding to the number clockwise in turn.

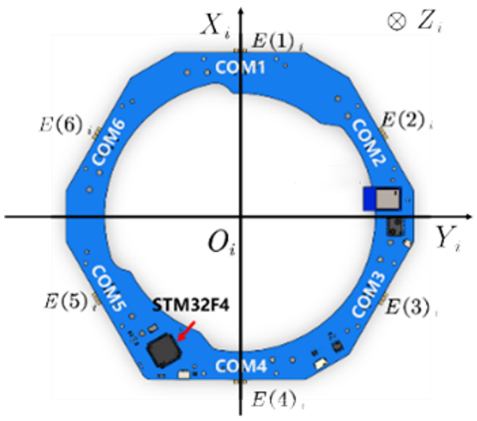

Figure 3. Communication module circuit board.

The module coordinate system S_i represents the

coordinate system of the i-th unit module, and the origin of the coordinate system coincides with the geometric center of the unit module. In the module coordinate system, the positive direction of the X_i axis is perpendicular to the connecting surface $E(1)$, the positive direction of the Y_i axis is between $E(2)_i$ and $E(3)_i$, and the positive direction of the Z_i axis is perpendicular to the paper face.

The description of topological relations in modular robots usually draws on the graph theory. That is using topology to describe the connection between nodes. The composition of the graph includes a non-empty finite set of nodes and a set of edges between nodes [14]. In the reconfigurable flight array, the connection surfaces in each unit module are used as nodes, and the two connected surfaces between different unit modules are used as edges. The configuration matrix is formed according to the topological connection relationship between nodes. The connection relationship between nodes is expressed as follows:

$$a_{ij} = \begin{cases} R(j)_k, & \lambda(j)_i = 1 \\ 0, & \lambda(j)_i = 0 \end{cases} \quad (1)$$
$$R(j)_k = j,\ k \neq i$$

where a_{ij} represents the serial port receiving data of the j-th connection surface in the i-th unit module. $R(j)_k$ represents the data sent by the serial port on the j-th connection surface in the k module and $\lambda(j)_i$ indicates whether the serial port interface on the j-th connection surface of the i-th module receives the data sent by the adjacent module. When the data is received, the value of $\lambda(j)_i$ is 1, the data is not received, and the value of $\lambda(j)_i$ is 0. The configuration matrix $C_{N\times6}$ is formed by a_{ij} as an element.

$$\mathbf{C}_{N\times6} = \begin{bmatrix} a_{11} & a_{12} & \cdots & a_{16} \\ a_{21} & a_{22} & \cdots & a_{26} \\ \vdots & \vdots & \ddots & \vdots \\ a_{N1} & a_{N2} & \cdots & a_{N6} \end{bmatrix} \quad (2)$$

The modular reconfigurable flight array has the phenomenon of isomorphic configuration. That is, although the reconfigurable flight array has the same configuration, but the configuration matrices of the two flight arrays are different. As shown in Figure 4.

The configuration matrix of the isomorphic four-rotor reconfigurable flight array is expressed by Formula (2):

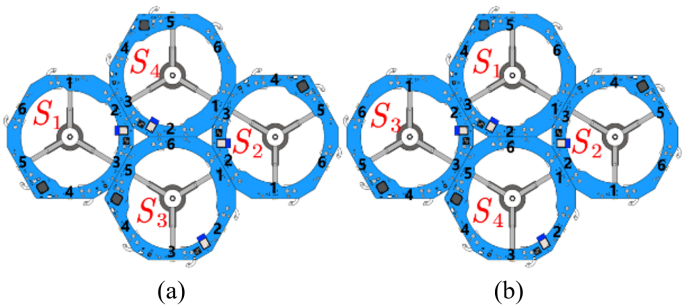

(a) (b)

Figure 4. Homogeneous quad-module reconfigurable flight array.

$$\mathbf{C}^a_{4\times6} = \begin{bmatrix} 0 & 3 & 5 & 0 & 0 & 0 \\ 0 & 1 & 1 & 0 & 0 & 0 \\ 2 & 0 & 0 & 3 & 0 & 2 \\ 3 & 6 & 2 & 0 & 0 & 0 \end{bmatrix} \mathbf{C}^b_{4\times6} = \begin{bmatrix} 3 & 6 & 2 & 0 & 0 & 0 \\ 0 & 1 & 1 & 0 & 0 & 0 \\ 0 & 3 & 5 & 0 & 0 & 0 \\ 2 & 0 & 0 & 3 & 0 & 2 \end{bmatrix} \quad (3)$$

It can be concluded that the value of the configuration matrix is determined by the serial port receiving data a_{ij} and the module number i of the unit module. Where a_{ij} can be solved by Formula (1). The number i of the flying array unit module is determined by the breadth-first search traversal algorithm based on the connection relationship between the unit modules. Finally, the topology of the reconfigurable flight array with any configuration is automatically updated accurately and efficiently, and the solved configuration matrix is uniquely corresponding to this configuration. The configuration matrix generation algorithm is shown in Algorithm 1 and Algorithm 2.

In the configuration identification, the main module begins to search and traverse the serial communication interface on each connection surface of each unit module, and finally realizes the automatic numbering of the slave module and the connection vector of the slave module is broadcast to the main module using the Bluetooth module. Finally, the configuration matrix of the reconfigurable flight array is obtained.

The implementation process of the main module configuration recognition algorithm is as follows:

Step 1: Sending instructions to the serial port of each connection surface.

Step 2: Waiting for all connection surfaces of each module in MRFA to send instructions successfully.

Step 3: The module determines the connection relationship and automatically generates the number according to whether it receives information from

Algorithm 1: Main module configuration recognition algorithm.

Input: The number of unit modules N, the connection vector a_k of the k-th module
Output: Configuration matrix $C_{N\times 6}$

$Mod.Num \leftarrow 1$ // The main module number is No. 1
for $j = 1$ **to** 6 **do**
  // The main module sends information to each connection surface
  $UART[j].Tx \leftarrow j$;
  $Mod.TxFlag[ID] \leftarrow 1$// The main module sends information to complete the flag
for $i = 1$ **to** 6 **do**
  // Waiting for each connection surface in each module to complete the information transmission
  while $Mod.TxFlag[i] \sim 1$ **do**
    $M \leftarrow 1$;
for $i = 1$ **to** 6 **do**
  // The module is automatically numbered according to the connection information
  if $UART[i].Rx = j$ *and* $M = 0$ **then**
    $M \leftarrow M + 1$;
    $a_1[i-1] \leftarrow j$;
  else
    $a_1[i-1] \leftarrow 0$;
$Num \leftarrow M$;
$Pub.Num \leftarrow Num$// Broadcast number information
$Pub.Mod[1].NumSuc \leftarrow 1$// Broadcast module execution status flag bit
while $a_N \neq NULL$ **do**
  $C_{N\times 6} \leftarrow [newRows, a_i]$// The connection vectors of each module are formed into a matrix form
return $C_{N\times 6}$

other unit modules.

Step 4: According to the connection information received by each connection surface, the main module connection vector is formed.

Step 5: The received connection vectors are summarized until the number of connection vectors is equal to the number of unit modules. Then the output configuration matrix $C_{N\times 6}$ is obtained.

From the module configuration recognition algorithm implementation process as follows:

Step 1: Sending instructions to the serial port of each connection surface.

Step 2: Waiting for the number to be completed. Moreover, the previous module completes the program execution and set the status flag as 1.

Step 3: The module determines the connection relationship and automatically generates the number according to whether it receives information from other unit modules.

Step 4: According to the connection information received by each connection surface, the connection vector is formed and sent it to the main module through Bluetooth broadcast.

Remark 1. Reconfigurable flight array unit module is composed of one main module and multiple slave modules. The hardware structure of the main module and the slave module is exactly the same, and the algorithm is different. Among them, the main module program corresponds to Algorithm 1, and the slave module program corresponds to Algorithm 2.

Remark 2. The number of the main module of the modular reconfigurable flight array is fixed and numbered $i = 1$, and the number of other slave unit modules is obtained by the breadth-first search traversal algorithm.

Remark 3. In the assembly process, it is necessary to ensure that the reconfigurable flight array includes one main module. The total number of modules is theoretically not limited.

According to the configuration matrix $C_{N\times 6}$ solved by the main module configuration identification algorithm in step 5 of Algorithm 1, the position $({}^{s_1}x_i, {}^{s_1}y_i)$ of each module in the reconfigurable flight array under the main module coordinate system S_1 can be calculated.

The coordinate of the i-th module in the main module coordinate system S_1 is $({}^{s_1}x_i, {}^{s_1}y_i)$, and the side length of the unit module is L. When the adjacent module is connected to the connection surface $E(j)_i$, its position can be expressed as:

$$\begin{cases} {}^{s_1}x_i + 2\cos\dfrac{\pi}{6}\cdot L\cdot\cos\left[(j-1)\cdot\dfrac{\pi}{3}\right] \\ {}^{s_1}y_i + 2\cos\dfrac{\pi}{6}\cdot L\cdot\sin\left[(j-1)\cdot\dfrac{\pi}{3}\right] \end{cases} \tag{4}$$

In the MRFA, each unit module has the same mass, i.e. $m_1 = m_2 = \cdots = m_N = m$. By solving the position

Algorithm 2: The k slave module configuration recognition algorithm.

Input: The number of numbered modules $Pub.Num$, the $k-1$ module execution status flag bit $Pub.Mod[k-1].NumSuc$, the connection information to determine the number M

Output: Configuration matrix $C_{N\times 6}$

for $j = 1$ **to** 6 **do**
  // Send information from each connection surface of the module
  $UART[j].Tx \leftarrow j$;
  $Mod.TxFlag[ID] \leftarrow 1$// The main module sends information to complete the flag bit
for $i = 1$ **to** 6 **do**
  // Wait for each connection surface in each module to complete the information transmission
  while $Mod.TxFlag[i] \sim 1$ **do**
    $M \leftarrow 1$;
for $i = 1$ **to** 6 **do**
  // The module is automatically numbered according to the connection information
  if $UART[i].Rx = j$ *and* $M = 0$ **then**
    $M \leftarrow M + 1$;
    $a_1[i-1] \leftarrow j$;
  else
    $a_1[i-1] \leftarrow 0$;
$Num \leftarrow M$;
$Pub.Num \leftarrow Num$// Broadcast number information
$Pub.Mod[1].NumSuc \leftarrow 1$// Broadcast module execution status flag bit
while $a_N \neq NULL$ **do**
  $C_{N\times 6} \leftarrow [newRows, a_i]$// The connection vectors of each module are formed into a matrix form
return $C_{N\times 6}$

$({}^{s_1}x_i, {}^{s_1}y_i)$ of each unit module in the main module coordinate system, the centroid coordinate $({}^{s_1}x_0, {}^{s_1}y_0)$ of the reconfigurable flight array in the main module coordinate system can be obtained as:

$$ {}^{s_1}x_0 = \frac{\sum_{i=1}^{N} {}^{s_1}x_i m_i}{\sum_{i=1}^{N} m_i}, \quad {}^{s_1}y_0 = \frac{\sum_{i=1}^{N} {}^{s_1}y_i m_i}{\sum_{i=1}^{N} m_i} \tag{5} $$

Because the mass of each unit module is the same, the formula (5) can be sorted out to obtain as:

$$ {}^{s_1}x_0 = \frac{\sum_{i=1}^{N} {}^{s_1}x_i}{N}, \quad {}^{s_1}y_0 = \frac{\sum_{i=1}^{N} {}^{s_1}y_i}{N} \tag{6} $$

where N represents the number of all unit modules.

By moving the coordinate system to the center of mass, the position of each unit module of the reconfigurable flight array can be calculated by the following formula (7).

$$ \begin{cases} Bx_i = {}^{s_1}x_i - {}^{s_1}x_0 \\ By_i = {}^{s_1}y_i - {}^{s_1}y_0 \end{cases} \tag{7} $$

In order to uniformly express the coordinates and attitudes of each unit module, the body coordinate system B is defined. The origin of the body coordinate system is located at the centroid position of the reconfigurable flight array. The coordinate system satisfies the right-hand rule, where the positive direction of the ${}^{B}X$-axis is the forward direction of the reconfigurable flight array, the positive direction of the ${}^{B}Z$-axis is perpendicular to the paper face, and the ${}^{B}Y$-axis direction is determined according to the right-hand rule. The forward direction of the reconfigurable flight array coincides with the X_1-axis direction of the main module coordinate system.

4 Dynamics model and controller design

In order to describe the motion relationship of the reconfigurable flight array in three-dimensional space, the world coordinate system W is defined. The world coordinate system satisfies the right-hand rule, and the X, Y, Z-axis follows the northeast sky (ENU) direction. The attitude information of the reconfigurable flight array includes the roll angle ϕ, pitch angle θ, and yaw angle ψ, which rotate around the x, y, z axes of the world coordinate system respectively.

In this paper, the modeling method in [16] is used to create a dynamic model of modular reconfigurable flight array. According to the relationship between lift, torque and motor speed, a general dynamic model of flight array with irregular structure is established.

$$ \begin{bmatrix} T_z \\ \tau_x \\ \tau_y \\ \tau_z \end{bmatrix} = \mathbf{L} \begin{bmatrix} 1 & 1 & \cdots & 1 \\ By_1 & By_2 & \cdots & By_N \\ -Bx_1 & -Bx_2 & \cdots & -Bx_N \\ (-1)^k & (-1)^k & \cdots & (-1)^k \end{bmatrix} \begin{bmatrix} \omega_1^2 \\ \omega_2^2 \\ \vdots \\ \omega_N^2 \end{bmatrix} \tag{8} $$

where T_z is the resultant force of the reconfigurable flight array in the body coordinate system, τ_x, τ_y, τ_z

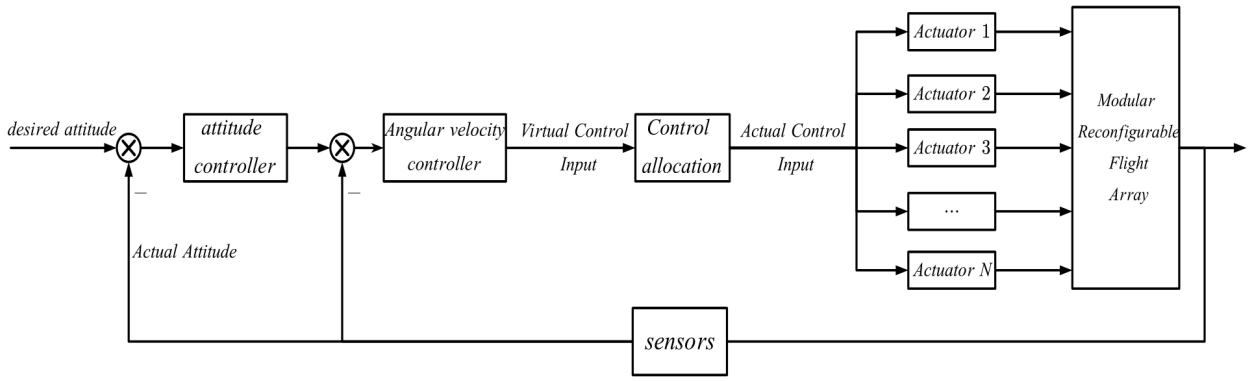

Figure 5. Reconfigurable flight array control diagram.

represents the rotational torque of the flight array rotating around the x_B, y_B, z_B-axis of the body coordinate system. ω_i denotes the rotation speed of the i-th propeller, and $\mathbf{L} = \text{diag}(L_f, L_f, L_f, L_m)$ is a constant diagonal matrix. k represents the rotation direction of the propeller in the flight array. When the propeller rotates clockwise $k = 1$, the propeller rotates counterclockwise $k = 2$.

Sorting out Equation (8), we have

$$\mathbf{u_v} = \mathbf{L}\mathbf{B_{CA}}\mathbf{u_m} \tag{9}$$

In this formula,$\mathbf{u_v} = [T, \tau_x, \tau_y, \tau_z]^T$ is the virtual control input, $\mathbf{u_m} = [\omega_1^2, \omega_2^2, \ldots, \omega_N^2]^T$ is the actual input of the flight array actuator, and $\mathbf{B_{CA}}$ denotes the control allocation matrix, which reflects the mapping relationship between the virtual control input and the actual input.

Finally, the Moore-Penrose pseudo-inverse is used to assign virtual control commands to each actuator.

$$\begin{aligned}\mathbf{u_m} &= \mathbf{B_{CA}^T}\left(\mathbf{B_{CA}}\mathbf{B_{CA}^T}\right)^{-1}\mathbf{L^{-1}}\mathbf{u_v} \\ &= \mathbf{B_{CA}^\dagger}\mathbf{L^{-1}}\mathbf{u_v}\end{aligned} \tag{10}$$

where $\mathbf{B_{CA}^\dagger}$ denotes the right pseudo-inverse of the control allocation matrix $\mathbf{B_{CA}}$.

Nowadays, many scholars use cascade proportional differential integral (PID) control [17, 18], active disturbance rejection control [19], fixed-time disturbance rejection control [15], and geometric tracking control method [20] for rotor UAV flight attitude control methods.

Methods such as active disturbance rejection control perform well in terms of immunity, but their design and tuning processes are relatively complex. Especially when dealing with highly dynamic flight arrays may bring additional computational burden. Geometric control methods can provide high accuracy in attitude tracking, but require high modelling accuracy and are susceptible to model uncertainty. In contrast, the cascade PID controller adopts a dual-loop structure to control the attitude and angular velocity separately, which enables it to exhibit excellent stability and response speed in dealing with complex multi-rotor flight arrays.

Consequently, a cascade PID control is used to realize the attitude control of reconfigurable flight array, which is divided into attitude control loop and angular velocity control loop. The cascade PID control algorithm obtains the control input according to the deviation between the given expected value $[\phi^*, \theta^*, \psi^*, p^*, q^*, r^*]^T$ and the current value $[\phi, \theta, \psi, p, q, r]^T$ collected by the sensor, and realizes the control of the reconfigurable flight array.

The PID control system for the attitude control of the reconfigurable flight array is shown in Figure 5.

5 Experiments

Take the configuration shown in Figure 6 as an example. A modular reconfigurable flight array is assembled and the configuration online identification and flight control are performed according to the designed algorithm to verify the effectiveness of the proposed algorithm.

5.1 On-line configuration identification

In the assembled modular reconfigurable flight array, the length of each side of the unit module is $L = 105mm$ and the quality is $m = 268g$. Module 1 is the main module, and the remaining unit modules are slave modules. The breadth-first search algorithm is used to automatically number the slave modules, and the numbering results of the unit modules are shown in Figure 6(b).

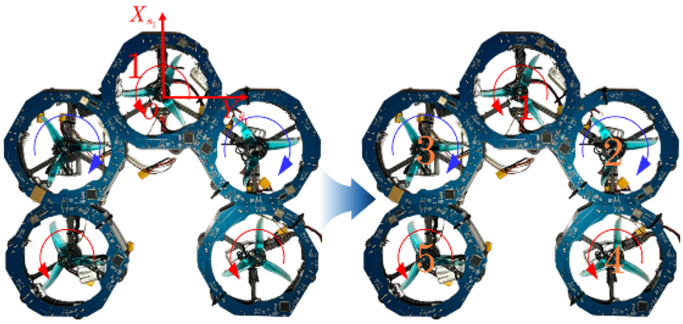

(a) (b)

Figure 6. Five-module reconfigurable flight array.

Finally, the Bluetooth module on the unit module is used to send the connection information of each slave module to the main module to form the configuration matrix $\mathbf{C_{5\times6}}$, and the configuration recognition of the reconfigurable flight array shown in Figure 6 is completed. The experimental results are as follows.

$$\mathbf{C}^{a}_{5\times6} = \begin{bmatrix} 0 & 0 & 4 & 0 & 2 & 0 \\ 0 & 1 & 0 & 3 & 0 & 0 \\ 0 & 5 & 0 & 2 & 0 & 0 \\ 2 & 0 & 0 & 0 & 0 & 0 \\ 0 & 4 & 0 & 0 & 0 & 0 \end{bmatrix} \tag{11}$$

From the configuration matrix and formula (4), the coordinates of each unit module in the main module coordinate system S_1 can be calculated, as shown in Table 1.

Table 1. The coordinates of each unit module in the main module coordinate system S_1.

Module number	1	2	3	4	5
${}^{s_1}x_i$ (mm)	0	-90.93	-90.93	-272.80	-272.80
${}^{s_1}y_i$ (mm)	0	157.5	-157.5	157.5	-157.5

The coordinates of the centre of mass in the main module coordinates S_1 are

$$\begin{cases} {}^{S_1}x_0 = -145.49 \\ {}^{S_1}y_0 = 0 \end{cases}$$

substituting the above results into Formula (7), the position coordinates of each module in the body coordinate system can be calculated. Details can be seen in Table 2.

In order to verify the feasibility of the algorithm for the isomorphic configuration phenomenon of the reconfigurable flight array, the master module program is downloaded into the unit module

Table 2. The coordinates of each unit module in the body module coordinate system B.

Module number	1	2	3	4	5
${}^{B}x_i = (mm)$	145.49	54.56	54.56	-127.31	-127.31
${}^{B}y_i = (mm)$	0	157.5	-157.5	157.5	-157.5

numbered 1 as shown in Figure 7(a), and the remaining modules are downloaded the slave program. Its configuration matrix is:

$$\mathbf{C}'_{5\times6} = \begin{bmatrix} 0 & 5 & 0 & 2 & 0 & 0 \\ 0 & 0 & 4 & 0 & 2 & 0 \\ 0 & 4 & 0 & 0 & 0 & 0 \\ 0 & 1 & 0 & 3 & 0 & 0 \\ 2 & 0 & 0 & 0 & 0 & 0 \end{bmatrix} \tag{12}$$

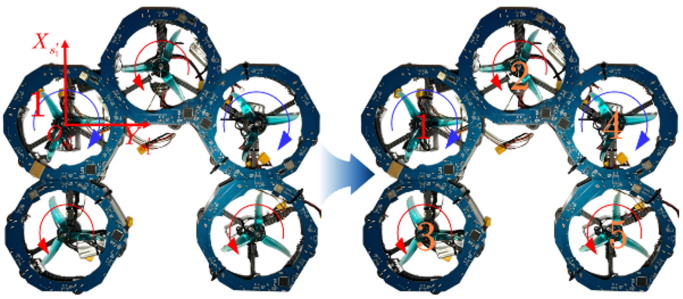

(a) (b)

Figure 7. Five-Module Reconfigurable Flight Array with Homogeneous Configuration.

where S'_1 represents the main module coordinate system, and the coordinates of the unit module within this system are provided in Table 3.

Table 3. The coordinates of each unit module in the body module coordinate system S'_1.

Module number	1	2	3	4	5
${}^{S_1}x_i = (mm)$	0	90.93	-181.87	0	-181.87
${}^{S_1}y_i = (mm)$	0	157.5	0	315.0	315.0

Its centroid coordinates in the main module coordinate system S'_1 are:

$$\begin{cases} {}^{S'_1}x_0 = -54.56 \\ {}^{S'_1}y_0 = 157.5 \end{cases}$$

Consequently, the positional coordinates of its unit modules under the body coordinate system are shown in Table 4.

Table 4. The coordinates of each unit module in the body module coordinate system B'.

Module number	1	2	3	4	5
${}^{B'}x_i = (mm)$	54.56	145.49	-127.31	54.56	-127.31
${}^{B'}y_i = (mm)$	-157.5	0	-157.5	157.5	157.5

From Table 2 and Table 4, it can be seen that for the homogeneous flight arrays, the relative geometric configuration of the corresponding unit modules in the body coordinate system is identical, which proves the uniqueness and correctness of the recognition results of the configuration recognition algorithm proposed in this paper.

The configuration information calculated by the configuration recognition algorithm is used to realize the online dynamic modeling of the reconfigurable flight array. The flight array configuration shown in Figure 6. After 15 configuration recognition experiments, the average online recognition time is 569.4ms, and the longest recognition time is 643ms. The recognition results of the configuration matrix are the same as those of matrix (11), that is, the correct recognition rate is 100%, which verifies the real-time and stability of the configuration recognition algorithm.

5.2 Flight control of MRFA

The MRFA with five modules uses a Pixhawk 6C controller to achieve flight control. The flight array actuator is a Tmotor F80 Pro DC brushless motor. The BLHeli electronic governor runs at a frequency of up to 48 MHz. The reconfigurable flight array is powered by a 4S lithium battery.

After obtaining the position coordinates of each module in the body coordinate system, the actual control input of the reconfigurable flight array can be calculated from Equation (10), and the speed ω of each actuator can be calculated.

The experiment uses the remote control input as the attitude angle expectation of the flight array. By inputting the set PID parameters (see Table 5) into the PID controller, the flight control of the flight array is finally realized.

The attitude tracking curve of the reconfigurable flight array is illustrated in Figure 8, where the red solid line represents the desired attitude angle and the blue dashed line reflects the actual attitude angle of the flight array. The corresponding flight experiment is shown in Figure 9. As seen in Figure 8, the desired attitude undergoes a significant change at $t = 32s$, and the reconfigurable flight array swiftly adjusts to track this change with high precision, demonstrating its ability to perceive its self-topological configuration in real time. This response also verifies the effectiveness of dynamically constructing a flight model based on the perception data and controlling the system through a cascade PID controller, allowing for accurate and

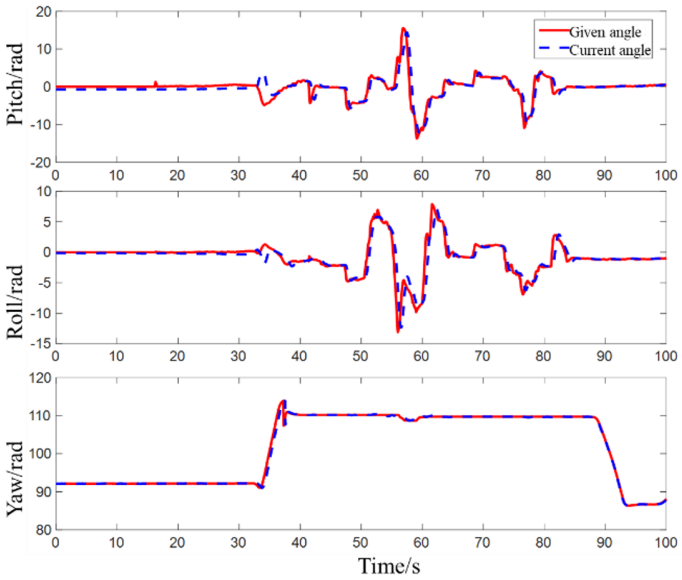

Figure 8. Attitude tracking curves of reconfigurable flight array.

Table 5. Cascade PID parameters of MRFA.

		P	I	D
Pitch	Angular velocity loop	1.4	0.27	0.0021
	Angle ring	4.7	0	0
Roll	Angular velocity loop	1.2	0.26	0.0025
	Angle ring	4.83	0	0
Yaw	Angular velocity loop	0.9	0.15	0
	Angle ring	5	0	0



Figure 9. Reconfigurable flight array flight experiments.

stable attitude tracking. Although this experiment was performed using only one specific configuration of the flight array, the proposed control algorithm is generalizable and ensures stable flight for various configurations such as six-rotor, seven-rotor, and eight-rotor systems. This versatility underscores the robustness of the algorithm, which can adapt to different modular configurations while maintaining reliable control and stable performance in all tested scenarios.

6 Conclusion

Based on the breadth-first search, this paper proposes the online automatic identification method for modular reconfigurable flight arrays with any configuration, and completes the calculation of the control allocation matrix of the reconfigurable flight array according to the identified configuration matrix. The accurate dynamic modeling of the corresponding configuration flight array helps the stable flight of the flight array greatly. Finally, the cascade PID control algorithm is used to realize the flight control of the reconfigurable flight array. The experimental results show that the configuration identification algorithm proposed in this paper can correctly calculate the configuration matrix of the flight array, and the configuration matrix is the premise of the control allocation matrix calculation. The stable flight of the flight array verifies the effectiveness of the controller, and also in turn verifies that the correct identification of the configuration matrix has a good role in promoting the modular reconfigurable flight array to achieve high-precision tracking flight performance. Moreover, optimal controller design based on on-line configuration identification mechanism will be discussed in our future work.

Data Availability Statement

Data will be made available on request.

Funding

This work was supported in part by the National Nature Science Foundation of China under Grant 62463014 and Grant 62273169; in part by the Yunnan Fundamental Research Projects under Grant 202301A and Grant T070401.

Conflicts of Interest

Jing Na served as an Editor-in-Chief, and Chunxi Yang served as an Associate Editor of the *ICCK Transactions on Intelligent Systematics* at the time of manuscript submission. To ensure the integrity of the peer-review process, neither Jing Na nor Chunxi Yang was involved in the editorial handling, peer review, or decision-making process for this manuscript, which was handled independently by another editor. The remaining authors declare no conflicts of interest.

Ethical Approval and Consent to Participate

Not applicable.

References

[1] Roussel, E., Gassmann, V., & Laroche, E. (2016, June). Modelling and identification of a coaxial birotor UAV from scarce flight data. In *2016 European Control Conference (ECC)* (pp. 2158-2164). IEEE. [CrossRef]

[2] Park, S., Lee, J., Ahn, J., Kim, M., Her, J., Yang, G. H., & Lee, D. (2018). Odar: Aerial manipulation platform enabling omnidirectional wrench generation. *IEEE/ASME Transactions on mechatronics*, 23(4), 1907-1918. [CrossRef]

[3] Zhou, X., Wen, X., Wang, Z., Gao, Y., Li, H., Wang, Q., ... & Gao, F. (2022). Swarm of micro flying robots in the wild. *Science Robotics*, 7(66), eabm5954. [CrossRef]

[4] Mu, B., & Chirarattananon, P. (2019). Universal flying objects: Modular multirotor system for flight of rigid objects. *IEEE Transactions on Robotics*, 36(2), 458-471. [CrossRef]

[5] Gabrich, B., Saldana, D., Kumar, V., & Yim, M. (2018, May). A flying gripper based on cuboid modular robots. In *2018 IEEE International Conference on Robotics and Automation (ICRA)* (pp. 7024-7030). IEEE. [CrossRef]

[6] Li, G., Gabrich, B., Saldana, D., Das, J., Kumar, V., & Yim, M. (2019, May). ModQuad-Vi: A vision-based self-assembling modular quadrotor. In *2019 International Conference on Robotics and Automation (ICRA)* (pp. 346-352). IEEE. [CrossRef]

[7] Oung, R., & D'Andrea, R. (2011). The distributed flight array. *Mechatronics*, 21(6), 908-917. [CrossRef]

[8] Carlson, S. J., Arora, P., & Papachristos, C. (2022, May). A multi-vtol modular aspect ratio reconfigurable aerial robot. In *2022 International conference on robotics and automation (ICRA)* (pp. 8-15). IEEE. [CrossRef]

[9] Zhao, N., Luo, Y., Wang, G., & Shen, Y. (2022). A deployable articulated mechanism enabled in-flight morphing aerial gripper. *Mechanism and Machine Theory*, 167, 104518. [CrossRef]

[10] Ryll, M., Bicego, D., & Franchi, A. (2016, October). Modeling and control of FAST-Hex: A fully-actuated by synchronized-tilting hexarotor. In *2016 IEEE/RSJ International Conference on Intelligent Robots and Systems (IROS)* (pp. 1689-1694). IEEE. [CrossRef]

[11] Ryll, M., Bicego, D., Giurato, M., Lovera, M., & Franchi,

A. (2021). Fast-hex—a morphing hexarotor: design, mechanical implementation, control and experimental validation. *IEEE/ASME transactions on mechatronics*, 27(3), 1244-1255. [CrossRef]

[12] Lau, H. Y. K., Ko, A. W. Y., & Lau, T. L. (2008). The design of a representation and analysis method for modular self-reconfigurable robots. *Robotics and Computer-Integrated Manufacturing*, 24(2), 258-269. [CrossRef]

[13] Yang, J., Yang, C., Zhang, X., & Na, J. (2024). Fixed-time sliding mode control with varying exponent coefficient for modular reconfigurable flight arrays. *IEEE/CAA Journal of Automatica Sinica*, *11*(2), 514-528. [CrossRef]

[14] Yu, H., Yu, J., Bi, S., & Zong, G. (2005). Configuration synthesis of reconfigurable robot based on graph theory. *Journal of Mechanical Engineering*, 41(8), 79-83. [CrossRef]

[15] Ma, D., Xia, Y., Shen, G., Jiang, H., & Hao, C. (2020). Practical fixed-time disturbance rejection control for quadrotor attitude tracking. *IEEE Transactions on Industrial Electronics*, 68(8), 7274-7283. [CrossRef]

[16] Mahony, R., Kumar, V., & Corke, P. (2012). Multirotor aerial vehicles: Modeling, estimation, and control of quadrotor. *IEEE robotics & automation magazine*, *19*(3), 20-32. [CrossRef]

[17] Bao, N., Ran, X., Wu, Z., Xue, Y., & Wang, K. (2017, December). Research on attitude controller of quadcopter based on cascade PID control algorithm. In *2017 IEEE 2nd Information Technology, Networking, Electronic and Automation Control Conference* (*ITNEC*) (pp. 1493-1497). IEEE. [CrossRef]

[18] Li, J., & Li, Y. (2011, August). Dynamic analysis and PID control for a quadrotor. In *2011 IEEE International Conference on Mechatronics and Automation* (pp. 573-578). IEEE. [CrossRef]

[19] Xu, L. X., Wang, Y. L., Wang, X., & Peng, C. (2023). Distributed active disturbance rejection formation tracking control for quadrotor UAVs. *IEEE Transactions on Cybernetics*, *54*(8), 4678-4689. [CrossRef]

[20] Lee, T., Leok, M., & McClamroch, N. H. (2010, December). Geometric tracking control of a quadrotor UAV on SE (3). In *49th IEEE conference on decision and control* (*CDC*) (pp. 5420-5425). IEEE. [CrossRef]



Bin Ren received the B.S. degree from the Shenyang Jianzhu University in 2018. He is currently working toward the M.S. degree at the Faculty of Mechanical and Electrical Engineering, Kunming University of Science and Technology. He research interests include modular reconfigurable aircraft attitude control, switch control, and its applications.



Jianhui Liu received the B.S. degree from the Kunming University of Science and Technology in 2021. She is currently working toward the M.S. degree in Kunming University of Science and Technology. Her research interest include heterogeneous UAV cluster control and path planning in space-constrained environments.



Simin Zhang received the BEng degree from Xi'an University in 2023.She is currently working toward the M.S. degree at the Faculty of Mechanical and Electrical Engineering, Kunming University of Science and Technology. She research interests include modular reconfigurable aircraft attitude control, Visual perception and reinforcement learning.



Chunxi Yang is a professor in the Faculty of Mechanical and Electrical Engineering, Kunming University of Science and Technology. He received his BE degree in process control from Qingdao University of Science and Technology, Qingdao, China, in 1999, ME degree from Wuhan Institute of Technology, Wuhan, China, in 2005, and PhD degree from Huazhong University of Science and Technology, Wuhan, China, in 2009. His main research interests are in the areas of networked control systems, distributed filtering and fusion, intelligent control system and process control.



Jing Na received the B.Sc. and Ph.D. degrees in automation and control from the School of Automation, Beijing Institute of Technology, Beijing, China, in 2004 and 2010, respectively. From 2011 to 2013, he was a Monaco/ITER Postdoctoral Fellow with ITER Organization, Saint-Paullez-Durance, France. From 2015 to 2017, he was a Marie Curie Fellow with the Department of Mechanical Engineering, University of Bristol, Bristol, U.K. Since 2010, he has been with the Faculty of Mechanical and Electrical Engineering, Kunming University of Science and Technology, Kunming, China, where he became a Professor in 2013. He has coauthored one monograph and more than 100 international journal articles and conference papers. His current research interests include intelligent control, adaptive parameter estimation, nonlinear control, and applications for robotics, vehicle systems, and wave energy converters. Dr. Na is currently an Associate Editor of the IEEE TRANSACTIONS ON INDUSTRIAL ELECTRONICS and the Neurocomputing, and has served as the Organization Committee Chair of Data Driven Control and Learning Systems Conference (DDCLS) 2019 and international program committee Chair of International Conference on Identification, Modeling and Control (ICMIC) 2017. He has been awarded the Best Application Paper Award of the third IFAC International Conference on Intelligent Control and Automation Science (IFAC ICONS 2013), and the Hsue-shen Tsien Paper Award, in 2017.